Gold nanoparticles surface-terminated with bifunctional ligands

Weili Shi[a], Y. Sahoo[b], Mark T. Swihart[a],*

[a] *Department of Chemical and Biological Engineering and Institute for Lasers, Photonics and Biophotonics,*
University at Buffalo (SUNY), Buffalo, NY 14260, USA
[b] *Department of Chemistry and Institute for Lasers, Photonics and Biophotonics, University at Buffalo (SUNY), Buffalo, NY 14260, USA*

Abstract

Gold nanoparticles have been prepared using bifunctional ligands of the type X−R−SH (X = −COOH, −OH, −NH$_2$) so that the surface is terminated with these functionalities. The ligands bind to the gold surface through their thiol (−SH end). The coverage and binding strength of the surfactant on the gold surface have been investigated using thermogravimetric analysis and FTIR spectroscopy. The nanoparticles appear to have excess surfactants on their surface, but these do not necessarily form a bilayer structure. The surfactant conformation allows enough room for the particles to be bonded to other surfaces, such as those of another nanoparticle, even with some excess surfactant present on their surface.
© 2004 Elsevier B.V. All rights reserved.

1. Introduction

Among colloids of metallic and semiconducting particles, gold colloid stands out as one of the most intensely investigated systems, with a history dating back to Faraday. This is primarily because it is chemically one of the most stable colloids [1]. Gold colloid can be prepared both in polar and in nonpolar media [2–5]. The facile two-phase synthesis method reported by Brust et al. was path breaking because it opened an entirely new route to understanding the stability, reactivity and self-assembly of metallic particles in nonpolar media [6]. In order that the novel electronic and optical properties of nanoparticles are fully exploited, it is desirable to have control of the growth of nanoparticle superstructures. It has been demonstrated by several groups that assembly of particles into one-, two- and three-dimensional configurations is feasible. One-dimensional chains of gold particles by template synthesis, self-assembly of two-dimensional arrays, and layer-by-layer assembly into three-dimensional ordered architectures are some noteworthy examples [7–10]. Controlled self-assembly techniques such as Langmuir–Blodgett layer-by-layer methods have made possible a host of interesting studies of topics including metal-insulator transitions, formation of nanotransistors, and construction of photonic crystals from these superstructures [11–13].

The formation of structures in a bottom-up self-assembly approach is governed by the polarity and reactivity of the nanoparticle surfaces. This is derived from the functionalization of the particle surfaces. The functionalities determine binding capabilities of the nanoparticles with other molecules, particles, and surfaces. A particularly elegant piece of recent work demonstrating highly specific functionalization is the binding of Au nanoparticles of two different sizes by a DNA linker demonstrated by Mirkin's group [14]. In this case, choosing an appropriate linker molecule was crucial so that the particles bind selectively into an ordered structure. On the other hand, it has been shown by Kiely et al. that thiol-stabilized gold particles in nonpolar solvents with a bimodal size distribution can organize themselves, without the necessity of a linker, into an ordered two-dimensional

---

* Corresponding author. Tel.: +1 716 645 2911x2205;
fax: +1 716 645 3822.
E-mail address: swihart@eng.buffalo.edu (M.T. Swihart).

arrays on solid surfaces [15]. The same group also demonstrated that two chemically different building blocks, namely thiol functionalized Au and Ag nanoparticles, can crystallize to form an ordered nanoscale alloy [16]. The crystallographic arrangement in these superlattices is hexagonal or cubic, depending on the ratio of particle radii. Clearly, there seems to be a parallelism between atomic scale intermetallic alloys and nanoscale alloy-like superlattices as the same geometric rules are followed. However, particle-solvent interaction and inter-particle interactions will have an important role in determining the morphology and the spatial extent of these ordered structures. Hence, in addition to particle size, changes in functionality on the particle surface and in solvent polarity can affect the superstructures formed.

In the present work, we present methods for preparing prototypical gold nanoparticle systems surface coated with bifunctional ligands of the type X–R–SH (X = –COOH, –OH, –NH$_2$). The gold surface is known to preferentially bind to the –SH group and hence the coated gold particles are expected to have –X termination [17]. We are especially interested in the stability of the particle dispersions, and hence in the coverage and binding strength of the surfactant on the gold surface through the –SH functionality. This has been investigated using thermogravimetric analysis and FTIR spectroscopy.

2. Experimental methods

The Au particles in this preparation are referred to according to their surface-binding ligands: 11-mercaptoundecanoic acid (Au–MUDA), 4-mercaptophenol (Au–MP), 1-mercaptohexanol (Au–MH) and 4-aminothiophenol (Au–ATP). Typical preparation procedures are given below.

2.1. Au–MUDA

An amount of 0.044 g 11-mercaptoundecanoic acid (MUDA) dissolved in 5 ml of methanol was added to 10 ml of 10 mM methanolic solution of HAuCl$_4$. The somewhat milky-looking mixture that resulted was vigorously stirred. After 20 min of stirring, 5 ml of freshly prepared 0.3 M aqueous sodium borohydride was added to the mixture dropwise with stirring. The reaction mixture turned deep brown indicating the formation of Au particles. The stirring was continued for one hour. The functionalized gold nanoparticles were retrieved from methanol by high-speed centrifugation and were subsequently redispersed in water. Excess surfactants and other ionic byproducts were removed by dialysis.

2.2. Au–MUDA (cold synthesis)

In this case, the sample was prepared in an ice bath (at 0 °C) and with a different concentration of precursors. 0.213 g MUDA dissolved in 20 ml of methanol was added to 20 ml of 5 mM methanolic HAuCl$_4$ with vigorous stirring, in a flask surrounded by an ice–water mixture. After 10 min of stirring,

40 ml of freshly prepared 0.39 M aqueous sodium borohydride was added to the mixture with stirring. The reaction mixture turned brown indicating the formation of Au particles. The stirring was continued for one hour. The functionalized gold nanoparticles were retrieved as described above.

2.3. Au–MP, Au–MH and Au–ATP

An amount of 0.018 g of 4-mercaptophenol, 0.033 g of 1-mercaptohexanol and 0.013 g of 4-aminothiophenol were dissolved in aliquots of 5 ml of methanol each and the procedures as above were followed. In all cases, deep brown-colored solutions were obtained indicating the formation of Au particles.

All the particles described are dispersible in water. However, Au–MP and Au–ATP disperse better in basic and acidic water, respectively.

3. Results and discussion

In this investigation, we select Au–MUDA as a model system for the binding of bifunctional surfactants onto the Au particle surface and present a more detailed analysis for it than for the other preparations.

The formation of Au particles in all cases was verified by UV–vis absorption spectroscopy, wherein the characteristic plasmon bands of Au particles are observed (Fig. 1). The bands appear in the expected wavelength region. The plasmon band of Au–MUDA prepared at reduced temperature is more prominent than others. The one for Au–ATP is slightly red shifted. Because of the propensity for intermolecular hydrogen bonding in these ligands, some particle aggregation and resultant broadening and red-shifting of the plasmon absorption peak are to be expected in all cases. This is most prominent in the case of Au–ATP. This is consistent with the TEM images shown in Fig. 2, where we find
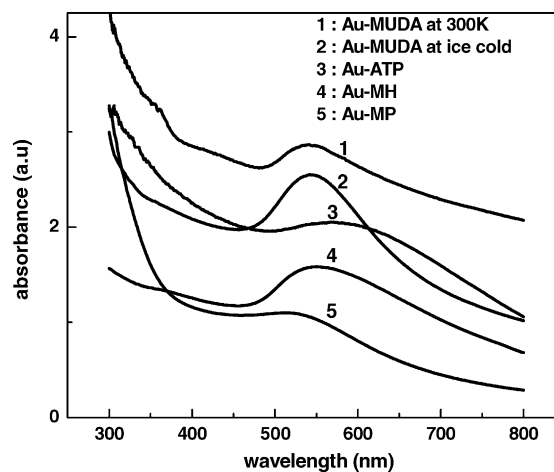

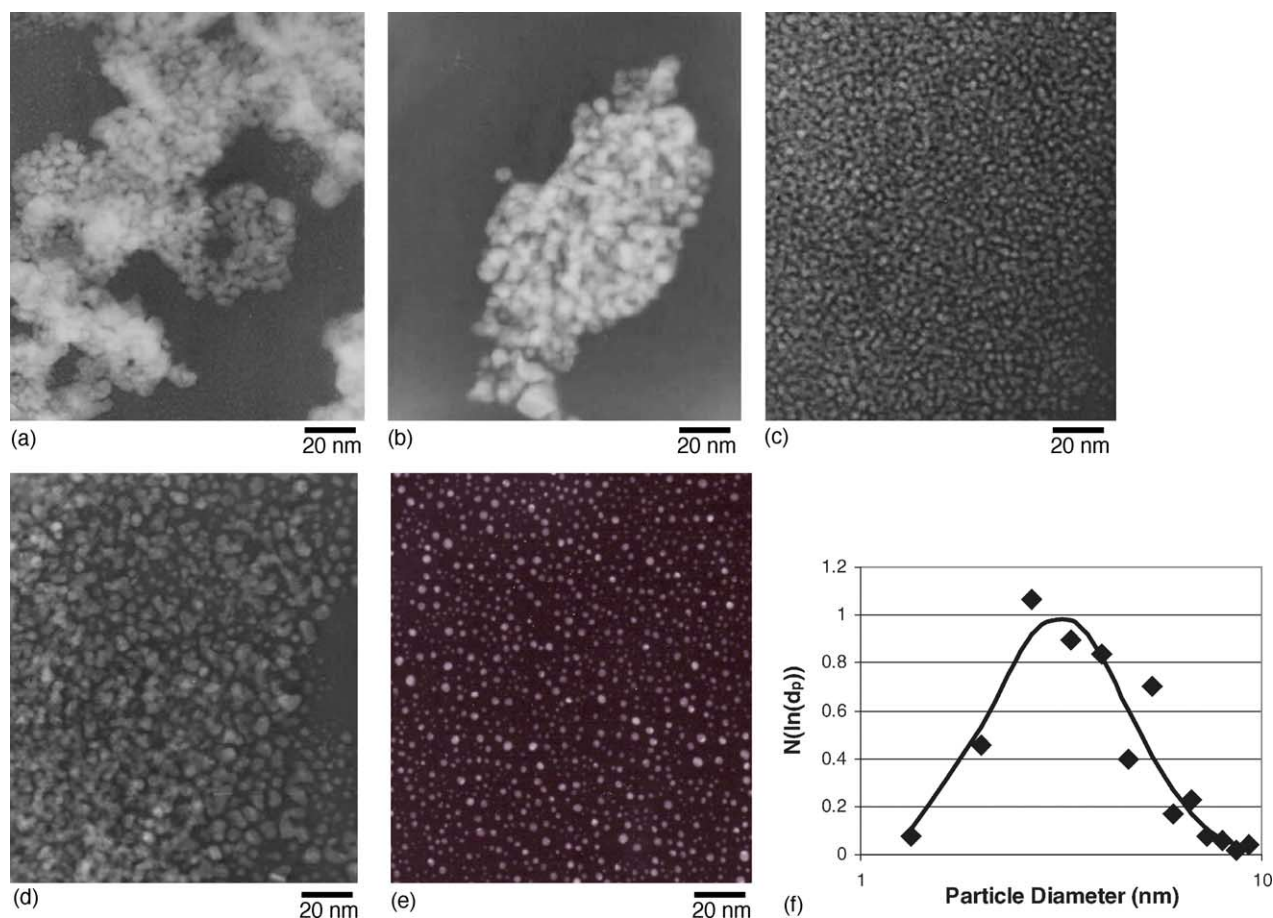Fig. 1. Visible absorption spectra of Au–MUDA (room temperature), Au–MUDA (ice-cold), Au–ATP, Au–MH and Au–MP.

Fig. 2. Transmission electron micrographs of (a) Au–MP, (b) Au–ATP, (c) Au–MH, (d) Au–MUDA (e) Au–MUDA(cold synthesis) and (f) size distribution of Au–MUDA in (d).

that agglomeration in the case of Au–ATP particles is more severe than in the others. The FTIR spectra for the Au particle samples were compared with those of the corresponding neat surfactants and it was found that the −SH stretching frequency (2550–2600 cm^{-1}) of the bound surfactants disappeared in all cases (as shown in Fig. 3 for MUDA versus Au–MUDA). This suggests that in all cases the bonding of the bifunctional ligands to the Au surface takes place through the −SH end. Further, the S−H bond is cleaved upon S−Au chemisorption, in agreement with the study done by Brust on the fate of sulfur-bound hydrogen during the formation of a thiol monolayer on gold [18]. We also note (Fig. 3) that the surfactant binding has an effect on the symmetric (d$^+$) and antisymmetric (d$^-$) stretching of the −CH$_2$ group. While there are minor shifts in frequencies (2–4 cm^{-1}), there is a significant narrowing of the peaks in the nanoparticle spectra. This is consistent with earlier studies where it has been argued that the rigid chain conformation on the nanoparticle surface generates a crystalline-like state of the chains and restricts their mobility, resulting in the narrowing of the stretching bands [19,20]. A notable point is the FTIR of Au–ATP (data not shown) where bonding to Au surface could potentially take place via either end of the ligand. We find that the −NH$_2$

band remains unchanged, which is consistent with the greater affinity of Au for −SH compared with −NH$_2$.

Thermogravimetric analysis (TGA) shows (Fig. 4) that the Au–MUDA starts losing mass at about 228 °C, which is

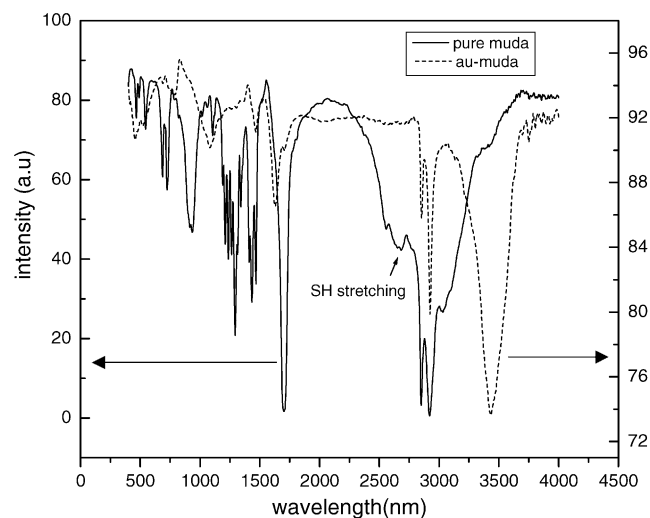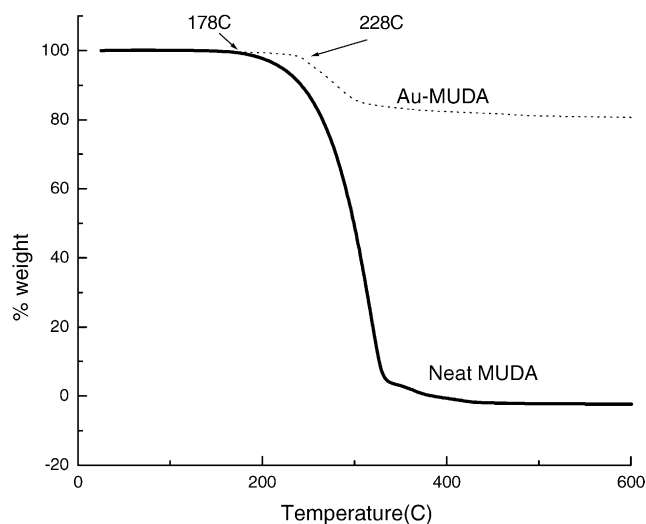Fig. 3. FTIR of Au–MUDA vs. neat MUDA.

Fig. 4. Thermogravimetric analysis curves for Au–MUDA and neat MUDA.

$50\,^{\circ}\mathrm{C}$ above the boiling point of MUDA. Past TGA studies of alkylthiol capped gold nanoclusters show that the weight loss occurs gradually, but more rapidly around the boiling point of the ligand [4,21]. Onset of weight loss at a higher temperature is a measure of the strength of chemisorption of MUDA onto the gold surface. The weight loss calculated from the curve is about 20%. We can rationalize the percentage weight loss by making an estimate of the ligand mass fraction in a polydisperse sample (with the size distribution shown in Fig. 2(f). If we assume a close-packed monolayer of the surfactant on the surface of a nanoparticle of diameter d_p then the total weight of the nanoparticle plus the monolayer is $(1/6)\pi d_p^3 \rho + (\pi d_p^2/a)(M/N_0)$ where d_p = the diameter of the particle, ρ = the density of the particle, a = the head area per molecule of the surfactant, M = the molecular weight of the surfactant, and N_0 = Avogadro number. Assuming that the TGA heating causes weight loss of only the surface-bound surfactant, the percentage weight loss from a particle of diameter d_p is $100 \times (\pi d_p^2/a)(M/N_0)/((1/6)\pi d_p^3 \rho + (\pi d_p^2/a)(M/N_0))$. For a polydisperse sample with size distribution $f(d_p)$, the total percentage weight loss is obtained by integrating over the size distribution:

$$\text{Percentage weight loss} = 100 \times \frac{\int\limits_0^\infty (\pi d_p^2/a)(M/N_0)f(d_p)\mathrm{d}d_p}{\int\limits_0^\infty ((1/6)\pi d_p^3 \rho + (\pi d_p^2/a)(M/N_0))f(d_p)\mathrm{d}d_p}$$

Fitting the nanoparticle size distribution observed in the TEM images for Au–MUDA to a lognormal form gave a log-mean particle diameter of 3.1 nm and a geometric S.D. of 1.5, as shown in Fig. 2(f). Integrating the above expression over this particle size distribution, using the bulk density of Au ($\rho = 19.3\,\mathrm{g/cm^3}$), parking area of thiol head group [22] ($a = 21\,\text{Å}^2$) and molecular mass of MUDA ($M = 218.36\,\mathrm{amu}$) gives the
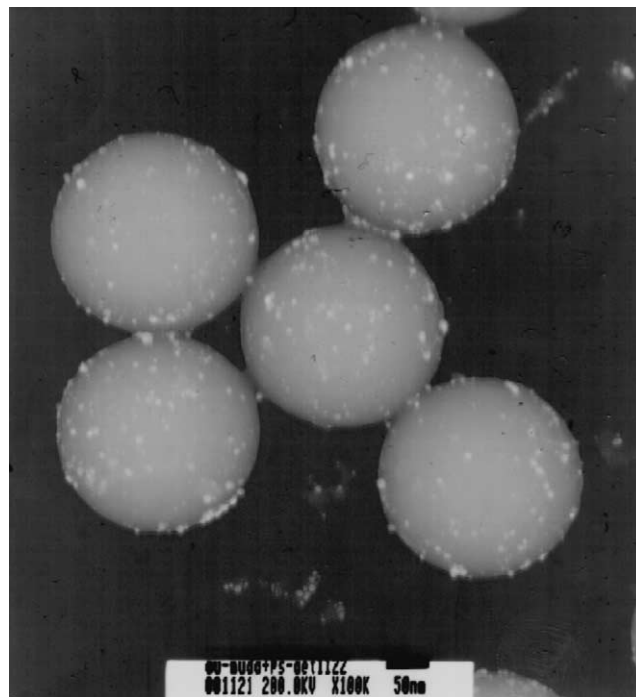

Fig. 5. TEM image of Au–MUDA attached to thiol-terminated polystyrene microspheres.

percentage weight loss for this particle size distribution as 10.2%. This value is lower than the weight loss observed from TGA (Fig. 4).

The above calculation suggests the presence of excess free surfactants. However, the absence of −SH stretching peak in the FTIR argues against this possibility. The most likely explanation of this apparent contradiction is that the lognormal distribution fit to the particle counting data from the TEM underestimates the number of small particles present.

Notwithstanding the use of sufficient surfactants, a close packed monolayer of these molecules on the highly curved surface of the nanoparticles may not be achieved. It is possible that the surfactants arrange themselves into close packed bunches (islands), leaving open spaces on the surface that can be susceptible to further bonding. This kind of chain conformation has been demonstrated by studying the dynamics of alkyl thiol on the surfaces of Au nanoparticles, by thermal and NMR studies [22,23]. We have tested this hypothesis by attempting to connect the Au–MUDA particles onto polystyrene particles. We stirred together aqueous dispersions of Au–MUDA nanoparticles and thiol-terminated polystyrene nanoparticles (296 nm), which should not bind to each other if the gold surface remains fully covered by MUDA. As shown in Fig. 5, the Au–MUDA particles actually did bind to the surface of the polystyrene which suggests that in spite of layered coverage by MUDA on the Au particles, there is still room on the particle surface for further bonding or that the surfactants can rearrange or be displaced to accommodate further bonding. As a control, Au–MUDA and polystyrene particles with carboxylic acid termination were

mixed together to test whether both the surface carboxylic acids could bind the particles together via hydrogen bonding, but there was no evidence of binding in the TEM images of those samples. However, after linking aminoethanthiol to the carboxylate group of these same polystyrene particles, the surface of the polystyrene is effectively thiol-terminated and the Au–MUDA nanoparticles bind, as evidenced in the TEM image in Fig. 5.

In summary, we have examined the surface functionalization and stability of Au nanoparticles prepared with various bifunctional ligands acting as surfactants. The sizes, discreteness and dipersability of the particles are influenced by the terminal functionality. Aqueous or polar solvent dispersibility of nanoparticles, in general, is beneficial for their use as catalysts, sensors, molecular markers, and drug delivery materials [23]. The presence of different terminal functionalities on the surface of nanoparticles provides a handle for further binding, either for creation of self-assembled structures or for attachment to biomolecules, co-catalysts, or other moieties of interest. In this study, we have examined the surface characteristics of Au nanoparticles by treating carboxylic terminal functionality as a model system. Mercaptoundecanoic acid (MUDA) binds to the surface of the particles in a specific manner both qualitatively and quantitatively, in spite of the copious amount used in an attempt to over-populate the surface. This provides enough room on the particle surface to enable particle binding on other thiol-terminated surfaces such as that of another particle.

Acknowledgements

References

[1] G. Schmid (Ed.), Clusters and Colloids, VCH, Weinheim, 1994.
[2] K.C. Grabar, P.C. Smith, M.D. Musick, J.A. Davis, D.G. Walter, M.A. Jackson, A.P. Guthrie, M.J. Natan, J. Am. Chem. Soc. 118 (1996) 1148.
[3] A.C. Templeton, S.W. Chen, S.M. Gross, R.W. Murray, Langmuir 15 (1999) 66.
[4] D.V. Leff, L. Brandt, J.R. Heath, Langmuir 12 (1996) 4723.
[5] M. Brust, J. Fink, D. Bethell, D.J. Schiffrin, C. Kiely, J. Chem. Soc., Chem. Commun. (1995) 1655.
[6] M. Brust, M. Walker, D. Bethell, D.J. Schiffrin, R. Whyman, J. Chem. Soc., Chem. Commun. (1994) 801.
[7] M. Trau, D.A. Saville, I.A. Aksay, Science 272 (1996) 706.
[8] L.C. Brousseau, S.M. Marinakos, J.P. Novak, D.L. Feldheim, Mater. Res. Bull. (1998) 129.
[9] T. Cassagneau, F. Guerin, J.H. Fendler, Langmuir 16 (2000) 7318.
[10] C.A. Foss, G.L. Hornyak, J.A. Stockert, C.R. Martin, J. Phys. Chem. 98 (1994) 2963.
[11] G. Markovich, C.P. Collier, J.R. Heath, Phys. Rev. Lett. 80 (1998) 3807.
[12] S.W. Chen, R.W. Murray, S.W. Feldberg, J. Phys. Chem. B 102 (1998) 9898.
[13] C. Graf, A. van Blaaderen, Langmuir 18 (2002) 524.
[14] R.C. Mucic, J.J. Storhoff, C.A. Mirkin, R.L. Letsinger, J. Am. Chem. Soc. 120 (1998) 12674.
[15] C.J. Kiely, J. Fink, M. Brust, D. Bethell, D.J. Schiffrin, Nature 396 (1998) 444.
[16] C.J. Kiely, J. Fink, J.G. Zheng, M. Brust, D. Bethell, D.J. Schiffrin, Adv. Mater. 12 (2000) 640.
[17] S.R. Johnson, S.D. Evans, R. Brydson, Langmuir 14 (1998) 6639.
[18] M. Hasan, D. Bethell, M. Brust, J. Am. Chem. Soc. 124 (2002) 1132.
[19] M.J. Hostetler, J.J. Stokes, R.W. Murray, Langmuir 12 (1996) 3604.
[20] Y. Sahoo, H. Pizem, T. Fried, D. Golodnitsky, L. Burstein, C.N. Sukenik, G. Markovich, Langmuir 17 (2001) 7907.
[21] R.H. Terrill, T.A. Postlethwaite, C. Chen, J.E. Hutchison, C. Poon, A. Tarzis, A. Chen, M.R. Clark, C.S. Johnson, E.T. Samulski, J.M. Desimone, R.W. Murray, Abstr. Papers Am. Chem. Soc. 210 (1995) 380.
[22] A. Badia, L. Cuccia, L. Demers, F. Morin, R.B. Lennox, J. Am. Chem. Soc. 119 (1997) 2682.
[23] D.E. Cliffel, F.P. Zamborini, S.M. Gross, R.W. Murray, Langmuir 16 (2000) 9699.